Shape reconstruction of 3D PEC: numerical results by the distributional approach

Aniello Buonanno, Raffaele Solimene, Rocco Pierri*

Department of Information Engineering, Second University of Naples, I-81031 Aversa, Italy,
* Ph.D. Student, e-mail aniello.buonanno@unina2.it

Abstract

The problem of determining the shape of three dimensional perfect electric conducting (PEC) objects from the scattered far-field under the incidence of plane waves with a fixed angle of incidence and varying frequency is dealt with. The Kirchhoff approximation is employed and the object's surface is represented as the support of a delta-distribution. Accordingly, the problem is cast as the inversion of a linear operator we deal with by means of the Truncated-Singular Value Decomposition. Numerical results are shown.

1.Introduction

In this contribution we consider the electromagnetic inverse scattering problem of imaging PEC objects from scattered field observations. Such a problem is relevant in a number of applicative contexts and as is well known is non-linear. Despite of that, it has been shown that, when the aim is to obtain "only" a "qualitative" reconstruction of the scatterers (in terms of their geometrical features) linear inversion schemes work well beyond the limits dictated by the linear models upon which they are based [1,2]. Following this result we exploit a linear inversion algorithm based on the Kirchhoff approximation. Moreover, we represent the object's surface as the support of a delta-distribution. This allows one to establish a linear integral relationship we invert by means of a Truncated Singular Value Decomposition (TSVD) scheme. Therefore, the present contribution can be considered as the extension to the 3D case of the approach presented in [1].
The inversion algorithm is checked against synthetic data which are generated independently from the model used to develop the inversion algorithm by means of the FEM software HFSS. Also data corrupted by an additive white Gaussian noise are considered.

2. Formulation of the problem and inversion algorithm

The geometry of the problem is shown in Fig. 1. A three-dimensional PEC scatterer whose surface is denoted with S is embedded in free space. The object is illuminated by y-polarized plane waves at different frequencies impinging along the z-axis, i.e., $\underline{E}_{inc} = E_0 \exp(-jk_0 z) i_y$ where i_x, i_y, i_z are the unit vectors of the Cartesian reference frame and k_0 is the wavenumber of the free space which ranges within the frequency band $[k_{0\min}, k_{0\max}]$. The scatterer's shape has to be retrieved from the scattered far-field collected for a *reflection-mode* configuration over a portion of a spherical domain concentric to the investigation domain and called the "observation domain". Through the Electrical Field Integral Equation we define the scattered electric far field as

$$\underline{E}^S(k_0,\underline{r}) = \begin{bmatrix} E_r^S(k_0,\underline{r}) \\ E_\theta^S(k_0,\underline{r}) \\ E_\varphi^S(k_0,\underline{r}) \end{bmatrix} = -j\omega\mu_0 \frac{\exp(-jk_0 r)}{4\pi r} \begin{pmatrix} 0 & 0 & 0 \\ \cos\theta\cos\varphi & \cos\theta\sin\varphi & -\sin\theta \\ -\sin\varphi & \cos\varphi & 0 \end{pmatrix} \iint_S \exp(jk_0 \underline{r}'\cdot\hat{r}) \begin{bmatrix} J_x(k_0,\underline{r}') \\ J_y(k_0,\underline{r}') \\ J_z(k_0,\underline{r}') \end{bmatrix} dS' \qquad (1)$$

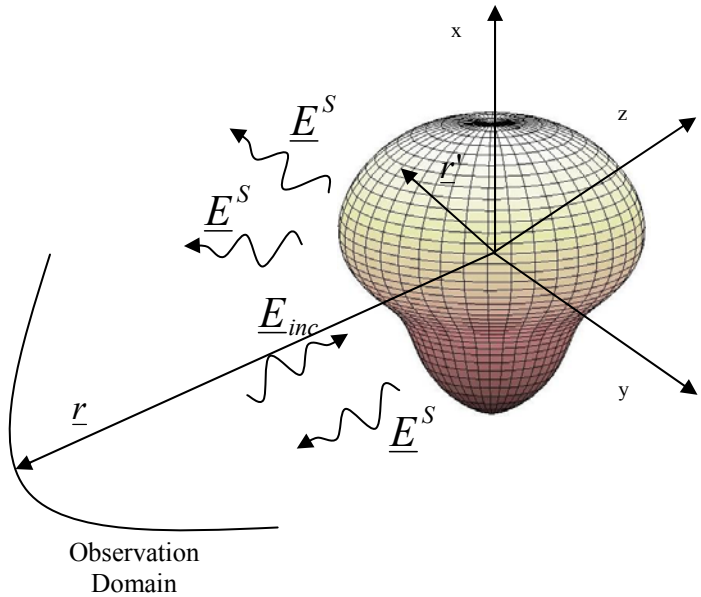

Figure 1 - Geometry of the problem

where $\underline{r}'$ and $\underline{r}$ are the position vectors of a point belonging to S and to the observation domain respectively, $\hat{r}$ is the direction of $\underline{r}$, $\underline{J}(k_0, \underline{r}')$ is the induced surface current density, θ and φ are the angles referring to observation point.

In eq. (1) the surface of the object, that is the unknown of the problem, coincides with the integration domain and the surface current density in turn depends on the unknown. The above relationship is linearized by resorting to the Kirchhoff approximation and the distributional formulation of the unknown. Accordingly, after some manipulations and by setting $u = -k_0 \sin\theta \cos\varphi$, $v = -k_0 \sin\theta \sin\varphi$ and $w = -k_0(\cos\theta - 1)$, eq. (1) can be approximated as

$$\underline{E}^S(k_0, \underline{r}) = \begin{bmatrix} E_\theta^S(k_0, \underline{r}) \\ E_\varphi^S(k_0, \underline{r}) \end{bmatrix} = \begin{pmatrix} \cos\theta \sin\varphi & -\sin\theta \\ \cos\varphi & 0 \end{pmatrix} \iiint_V \exp[-j(ux + vy + wz)] \begin{bmatrix} \gamma_z \\ \gamma_y \end{bmatrix} dV \tag{2}$$

where V is the investigation domain within we a priori known that the scatterer resides, the nonessential factor $-j\omega\mu_0 \frac{\exp(-jk_0 r)}{4\pi r} \frac{2}{\xi_0} E_0$ has been normalized and ξ_0 is the wave impedance of free space. Moreover,

$$\begin{cases} \gamma_y = (\hat{n}' \cdot i_y) U(-\hat{n}' \cdot i_z) \delta_S(\underline{r}) \\ \gamma_z = -(\hat{n}' \cdot i_z) U(-\hat{n}' \cdot i_z) \delta_S(\underline{r}) \end{cases} \tag{3}$$

$U(\cdot)$ is the Heaviside function accounting for the shadow boundary and the distribution $\delta_S(\underline{r})$ is defined as

$$\iiint_V \delta_S(\underline{r}) f(\underline{r}) d\underline{r} = \iint_S f(\underline{r}) dS \tag{4}$$

We observe that the eq. (2) has "only" two unknowns (γ_y and γ_z) whereas in general (see eq. (1)) the unknowns are three. This is resulted by the particular choice of polarization of the incident plane wave.

Accordingly, now, our problem amounts to invert the linear operator

$$A:\gamma_y,\gamma_z \in V' \rightarrow \left(E_\theta^S = \cos\theta \sin\varphi F_V \gamma_z - \sin\theta F_V \gamma_y, E_\varphi^S = \cos\varphi F_V \gamma_z\right) \in L_2^2(O) \tag{5}$$

where V' is the set of distributions whose supports are in V, F_V is the Fourier transform operator compactly supported over V and $L_2^2(O)$ is the Hilbert space composed of vectors of complex functions $\underline{g} = (g_\theta, g_\varphi)$ defined on O where g_θ and g_φ belong to the set of square integrable functions $L^2(O)$. The latter is the domain where the scattered field is observed. In particular for the multifrequency/singleview reflection-mode configuration $O = [\varphi_{\min}, \varphi_{\max}] \times [\theta_{\min}, \theta_{\max}] \times [k_{0\min}, k_{0\max}]$.

To perform the inversion of eq. (5) we extend to the present three-dimensional problem the two step based inversion algorithm exploited for the case of cylindrical scatterers [1]. First we achieve the reconstruction of only γ_z. This is advantageous from the computational point of view. In this hypothesis we obtain a scalar problem and the eq. (5) reduces to

$$A:\gamma_z \in V' \rightarrow E_\varphi^S = \cos\varphi F_V \gamma_z \in L^2(O) \tag{6}$$

Hence, in the first step γ_z is reconstructed by inverting eq. (6) by means of a TSVD procedure. This allows to obtain a stable (with respect to the noise) reconstruction. In the second step we will exploit the *a priori* information that the unknown γ_z is a distribution with positive real density by taking only the positive real parts of the reconstructions and introducing a suitable threshold [2]. In particular, the threshold is introduced with the aim of curtailing spurious artifacts which are due to smoothing of the regularization procedure and to the noise.

3. Numerical Results

In this section we report numerical reconstructions obtained by exploiting synthetically generated "*exact*" data thanks to the commercial FEM based HFSS tool, so that the inverse crime is avoided. Moreover, also a case with data corrupted by an AWG noise with zero mean and standard deviation so that to obtain a Signal to Noise Ratio (SNR) of 15 dB is shown.

In particular, the reconstructions have been obtained for $\theta \in [\pi/2, \pi]$rad, $\phi \in [0, 2\pi]$rad and $k_0 \in [4\pi, 8\pi]$m^{-1}. As investigation domain we considered $V = [-x_m . x_m] \times [-y_m . y_m] \times [-z_m . z_m]$, with $x_m = y_m = z_m = 2\lambda_{\max}$. The first reconstruction example is reported in Fig. 2 where we consider a PEC bounded plane of size $\lambda_{\max} \times \lambda_{\max}$ whose center is located at the origin of reference frame. As can be seen, the scatterer is very well localized and the shape is well reconstructed. As a further example, we test the inversion algorithm for the cases of Fig. 3 where a spherical PEC scatterer of radius $\lambda_{\max}$, located at the center of the reference system with data corrupted by AWGN as above explained, is considered. Also in this cases the scatterer is very well localized and the shape, of course only the illuminated side, is reconstructed.

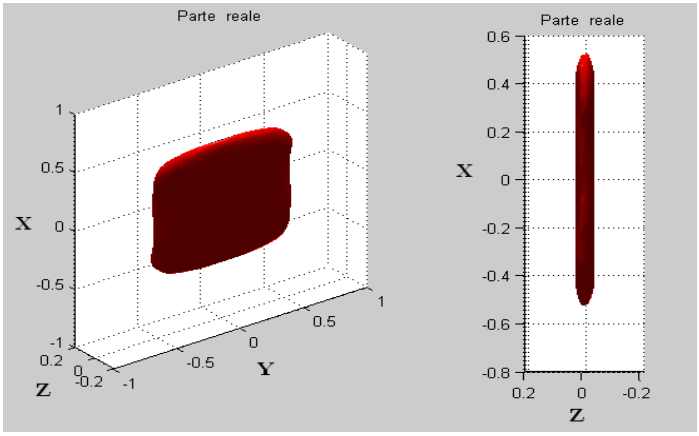

Fig. 2 - Normalized isosurface reconstruction of the plane scatterer. The axis are expressed in meter [m].

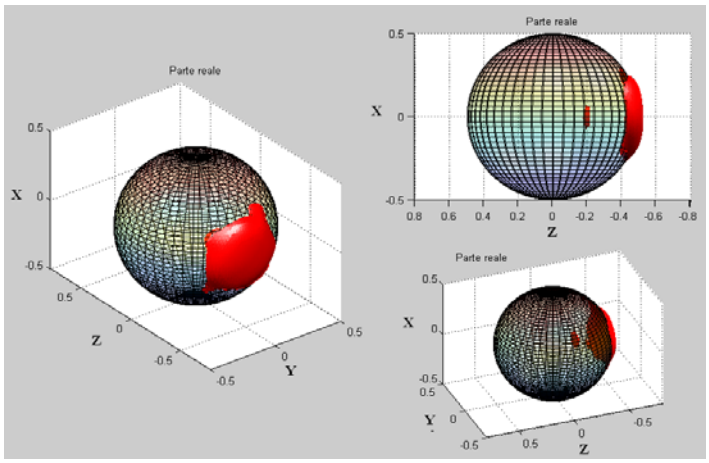

Fig. 3 - Normalized isosurface reconstruction of a PEC sphere of radius λ_{max} . Data are corrupted by AWG noise. The axis are expressed in meter [m].

4. References

1. R. Pierri, A. Liseno, R. Solimene, and F. Soldovieri, "Beyond physical optics SVD shape reconstruction of metallic cylinders," *IEEE Transactions on Antennas and Propagation*, vol. 54, pp. 655-665, 2006.

2. R. Solimene, A. Buonanno, and R. Pierri, "Imaging *small* PEC spheres by a linear δ approach", in print on *IEEE Transactions on Geoscience and Remote Sensing* .